

Optimal sliding friction coefficient for isolated bridges in different soil conditions

Original

Optimal sliding friction coefficient for isolated bridges in different soil conditions / Castaldo, Paolo; Ripani, Marianela; Lo Priore, Rosa. - ELETTRONICO. - 3:(2019), pp. 4864-4886. (Intervento presentato al convegno COMPDYN Congress 2019 - Computational Methods in Structural Dynamics and Earthquake Engineering tenutosi a Crete Island, Greece nel 24 - 26 June 2019).

Availability:

This version is available at: 11583/2776612 since: 2020-02-19T12:09:07Z

Publisher:

COMPDYN Congress 2019

Published

DOI:

Terms of use:

openAccess

This article is made available under terms and conditions as specified in the corresponding bibliographic description in the repository

Publisher copyright

(Article begins on next page)

OPTIMAL SLIDING FRICTION COEFFICIENT FOR ISOLATED BRIDGES IN DIFFERENT SOIL CONDITIONS

P. Castaldo¹, M. Ripani², and R. Lo Priore³

¹ Department of Structural, Geotechnical and Building Engineering (DISEG)
Politecnico di Torino, Turin, Italy
e-mail: paolo.castaldo@polito.it

² Universidad de Buenos Aires. Consejo Nacional de Investigaciones Científicas y Técnicas (CONICET). Instituto de Tecnologías y Ciencias de la Ingeniería “Hilario Fernández Long” (INTECIN). Facultad de Ingeniería
Buenos Aires, Argentina
mripani@fi.uba.ar

³ Department of Civil Engineering, University of Salerno
Fisciano, SA, Italy
r.lopriore@hotmail.it

Abstract

The work evaluates the optimal properties of friction pendulum system (FPS) bearings for the seismic protection of bridge piers under earthquake excitations having different frequency characteristics representative of different soil conditions in order to reduce the seismic vulnerability of infrastructures. A two-degree-of-freedom model is adopted to describe, respectively, the response of the infinitely rigid deck isolated by the FPS devices and the elastic behavior of the pier. By means of a non-dimensional formulation of the motion equations, a wide parametric analysis for several structural parameters is carried out. Seismic excitations, modelled as time-modulated filtered Gaussian white noise random processes having different intensities and frequency contents, are considered. Specifically, the filter parameters, which control the frequency contents, are properly calibrated to reproduce stiff, medium and soft soil conditions, respectively. Finally, the optimum values of the sliding friction coefficient able to minimize the pier displacements with respect to the ground are derived as a function of the structural properties, of the seismic input intensity and of the soil condition.

Keywords: Bridge, Seismic Isolation, Soil Condition, Performance, Optimal friction coefficient.

1 INTRODUCTION

Seismic isolation of bridges makes it possible to uncouple the deck from the horizontal components of the earthquake motion, leading to a substantial reduction of the deck acceleration and, consequently, of the forces transmitted to the pier [1]-[4]. In the last years, friction pendulum system (FPS) devices have often been preferred to other isolators for their capability of providing an isolation period independent of the mass of the supported structure, their capacity to assure high dissipation and recentering, and their longevity and durability properties [5]-[12]. In [13], with reference to an equivalent two-degree-of-freedom (2dof) model for base-isolated building frames, a non-dimensionalization of the motion equation considering different isolator and system properties has been proposed. Contextually, other studies have been focused on the seismic response of bridge isolated with sliding pendulum isolators highlighting the advantages [14]-[15]. Moreover, other works have been more oriented to develop design approaches for the isolators and to identify the optimal isolator properties. In this context, the seismic reliability-based design (SRBD) approach has been proposed and widely discussed in [16]-[22] as a new methodology useful to provide design solutions for seismic devices taking into account the main uncertainties relevant to the problem. Jangid [23], assuming a stochastic model of the earthquake ground motion, considered the seismic performance of a bridge equipped with FPS devices, characterized by a Coulomb behavior, illustrating that there exists an optimal value of the friction coefficient for which the pier base shear and deck acceleration can be minimized. Other works (e.g., [24]-[26],[27]) concerning isolated bridges have also demonstrated that soft soil condition leads to a higher demand in terms of displacements and shear forces by negatively influencing the isolated systems. In [28], the optimal values of the friction coefficient taking into account the influence of the ground motion characteristics by means of the ratio between the Peak Ground Acceleration (PGA) and the Peak Ground Velocity (PGV) have been proposed.

This work investigates the influence of soil characteristics in terms of frequency content on the seismic performance of bridges isolated with FPS isolators to define the optimal sliding friction coefficients. The two-degree-of-freedom model, as employed in [14],[29] is used for this purpose as an equivalent model representative of the dynamic behaviour of a single-column bent viaduct to describe, respectively, the seismic response of the infinitely rigid deck isolated by the FPS devices and of the elastic behavior of the pier. In compliance with the non-dimensionalization of the motion equations presented for base-isolated building frames in [13], in this study, a non-dimensionalization of the motion equations for isolated bridges is proposed in order to carry out a wide parametric analysis considering different values of the structural properties and three different sets of artificial ground motion records. These latter ones are modelled as non-stationary stochastic processes and generated through the power spectral density method [30], with different frequency contents corresponding to stiff, medium and soft soil conditions [31], respectively. Specifically, for each set of the random excitations, numerical simulations are executed to estimate the influence of the characteristic system and isolator properties on the response parameters relevant to the structural performance. Then, the optimal values of the sliding friction coefficient, able to minimize the pier displacements relative to the ground, are defined as a function of the structural parameters, of the seismic input intensity and of the soil condition.

2 NON-DIMENSIONAL MOTION EQUATIONS FOR ISOLATED BRIDGES

Assuming an equivalent 2dof model, the motion equations governing the response of a bridge equipped with single concave FPS devices (Figure 1), subjected to the seismic input $\ddot{u}_g(t)$, apply:

$$\begin{aligned} m_d \ddot{u}_d(t) + m_d \ddot{u}_p(t) + c_d \dot{u}_d(t) + f_b(t) &= -m_d \ddot{u}_g(t) \\ m_p \ddot{u}_p(t) - c_d \dot{u}_d(t) + c_p \dot{u}_p(t) + k_p u_p(t) - f_b(t) &= -m_p \ddot{u}_g(t) \end{aligned} \quad (1a,b)$$

where u_d denotes the displacement of the deck relative to pier, u_p the pier displacement relative to the ground, m_d and m_p respectively the mass of the deck and of the pier bridge, k_p and c_p respectively the pier stiffness and inherent viscous damping coefficient, c_d the bearing viscous damping factor, t the time instant, the dot differentiation over time, and $f_b(t)$ indicates the FPS force, that can be evaluated as:

$$f_b(t) = k_d u_d(t) + \mu(\dot{u}_d) m_d g \operatorname{sgn}(\dot{u}_d) \quad (2)$$

where $k_d = W / R = m_d g / R$, g is the gravity constant, R is the radius of curvature of the FPS, $\mu(\dot{u}_d(t))$ the sliding friction coefficient, which depends on the bearing slip velocity $\dot{u}_d(t)$, and $\operatorname{sgn}(\cdot)$ denotes the sign function. It follows that, similarly to base-isolated structures [13], the fundamental vibration period of an isolated bridge, $T_d = 2\pi\sqrt{R/g}$, corresponding to the pendulum component, is independent of the deck mass and related only to the radius of curvature R .

According to [8]-[10], the sliding friction coefficient of teflon-steel interfaces can be expressed as:

$$\mu(\dot{u}_d) = f_{\max} - Df \cdot \exp(-\alpha |\dot{u}_d|) \quad (3)$$

where f_{\max} and $f_{\min} = f_{\max} - Df$ represent, respectively, the maximum value of sliding friction coefficient attained at large velocities and the value at zero velocity. In this study, it is considered that $f_{\max} = 3f_{\min}$ with the exponent α equal to 30 [13]. Considering the maximum value of the sliding friction coefficient, the effective stiffness of the FPS bearings $k_{\text{eff}} = W(1/R + f_{\max}/u_d)$ as well as the corresponding effective isolated period $T_{d,\text{eff}}$ [32],[33] (Fig. 1) can be computed depending on the displacement demand. Note that Eqn.(1) does not consider the effects of the higher modes due to flexibility of the pier and is verified if only the horizontal component of the bearing displacement is considered [18] (i.e., high radii of curvature R). Furthermore, the equivalent 2dof model [14],[29] can be assumed representative of the dynamic behaviour of a single-column bent viaduct as long as the bridge is straight and consists of a large number of equal spans, of piers with equal height/stiffness and considering a superstructure (deck) that can be assumed to move as a rigid body [34].

Let us introduce the time scale $\tau = t\omega_d$ in which $\omega_d = \sqrt{k_d/m_d}$ is the fundamental circular frequency of the isolated system with infinitely rigid superstructure, and the seismic intensity scale a_0 , expressed as $\ddot{u}_g(t) = a_0 \ell(\tau)$ where $\ell(\tau)$ is a non-dimensional function of time describing the seismic input time-history, the following non-dimensional equations can be obtained and herein proposed for isolated bridges:

$$\begin{aligned} \ddot{\psi}_d(\tau) + \ddot{\psi}_p(\tau) + 2\xi_d \dot{\psi}_d(\tau) + \psi_d(\tau) &= -\ell(\tau) - \frac{\mu(\dot{\psi}_d)g}{a_0} \operatorname{sgn}(\dot{\psi}_d) \\ \ddot{\psi}_p(\tau) - \frac{1}{\lambda} \left[2\xi_d \dot{\psi}_d(\tau) + \psi_d(\tau) + \frac{\mu(\dot{\psi}_d)g}{a_0} \operatorname{sgn}(\dot{\psi}_d) \right] &+ 2\xi_p \frac{\omega_p}{\omega_d} \dot{\psi}_p(\tau) - \frac{\omega_p^2}{\omega_d^2} \psi_p(\tau) = -\ell(\tau) \end{aligned} \quad (4a,b)$$

where $\omega_p = \sqrt{k_p / m_p}$ and $\xi_p = c_p / 2m_p\omega_p$ represent respectively the circular frequency and damping factor of the pier bridge; $\omega_d = \sqrt{k_d / m_d} = \sqrt{g / R}$ and $\xi_d = c_d / 2m_d\omega_d$ are respectively the circular frequency and the isolator damping factor of the FPS isolator; $\lambda = m_p / m_d$ [14],[29],[32] the mass ratio. The non-dimensional parameters $\psi_d = \frac{u_d\omega_d^2}{a_0}$ and $\psi_p = \frac{u_p\omega_d^2}{a_0}$ describe the dynamic response of the deck and the pier, respectively. From Eqn.(4), it is possible to observe that the five non-dimensional Π terms [13],[35]-[36] that govern the system non-dimensional response are:

$$\Pi_\omega = \frac{\omega_p}{\omega_d}, \Pi_\lambda = \lambda, \Pi_\mu(\dot{\psi}_d) = \frac{\mu(\dot{u}_d)g}{a_0}, \Pi_{\xi_d} = \xi_d, \Pi_{\xi_p} = \xi_p \quad (5a,b,c,d,e)$$

where Π_ω represents the isolation degree [32],[37], Π_λ is the mass ratio as previously defined, Π_{ξ_p} and Π_{ξ_d} are related to the inherent viscous damping of the pier and the isolator, respectively, Π_μ denotes the isolator strength which depends on both the friction coefficient $\mu(\dot{u}_d)$ and the seismic intensity. Since the sliding friction coefficient is a velocity-dependent parameter, Π_μ is considered as follows [13]:

$$\Pi_\mu^* = \frac{f_{\max}g}{a_0} \quad (6)$$

From Eqn.s(4)-(6), note that only the non-dimensional terms $\Pi_{\xi_d}, \Pi_{\xi_p}, \Pi_\omega, \Pi_\lambda, \Pi_\mu^*$, the function $\ell(\tau)$, describing the frequency content and time-modulation of the seismic input, and the time scale parameter ω_d influence the non-dimensional seismic response of the bridge system isolated by FPS.

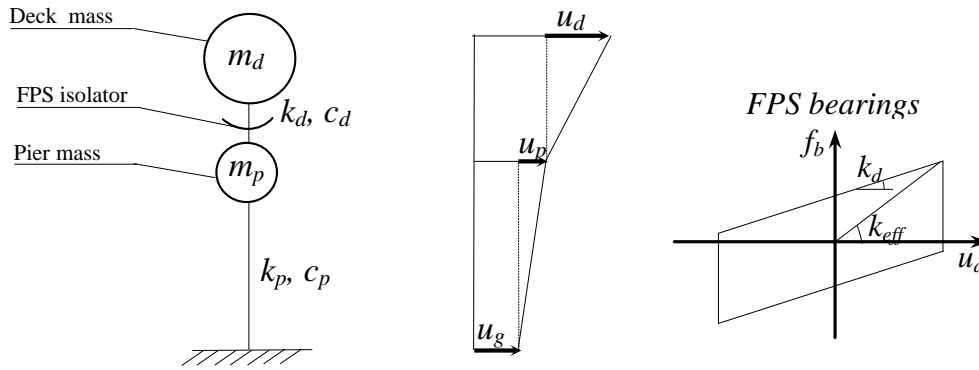


Figure 1: 2dof model of a bridge isolated by FPS bearings.

3 UNCERTAINTIES RELATED TO THE SEISMIC INPUT

This section describes the stochastic model employed for the generation of the artificial ground motions in order to reproduce the uncertainty in terms of frequency characteristics for different soil conditions as well as the uncertainty corresponding to the seismic intensity.

3.1 Random excitations

The "record-to-record" variability in terms of the dynamic characteristics of different seismic inputs related to stiff, medium and soft soil conditions, respectively, is herein described by means of three corresponding wide groups of artificial records having different frequency contents. These artificial inputs are modelled as time-modulated filtered Gaussian white noise random processes [30],[38] within the power spectral density (PSD) method [39] by adopting the Kanai-Tajimi model [40]-[41], modified by Clough and Penzien [42],[26],[43]-[53], as follows:

$$S_f(\omega) = \frac{\omega_g^4 + 4\xi_g^2\omega_g^2\omega^2}{(\omega_g^2 - \omega^2) + 4\xi_g^2\omega_g^2\omega^2} \cdot \frac{\omega^4}{(\omega_f^2 - \omega^2) + 4\xi_f^2\omega_f^2\omega^2} S_0 \quad (7)$$

in which S_0 is the amplitude of the bedrock excitation spectrum, modeled as a white noise process; ω_f and ξ_f are the Clough-Penzien filter parameters assumed as deterministic values, set equal to $\omega_f = 1.6$ (rad/s) and $\xi_f = 0.6$; ω is the circular frequency, assumed varying in the range 0 and 50 rad/s; ω_g and ξ_g represent the fundamental circular frequency and damping factor of the soil, respectively, assumed as uniformly distributed independent random variables with appropriate ranges of variation [31],[54] as follows: ω_g varies in the range 5π - 9π rad/s (high frequency/short period) with $\xi_g = 0.6$ -1 for stiff soil condition, ω_g is assumed ranging between 3π rad/s and 5π rad/s (intermediate frequency/ period) with $\xi_g = 0.4$ -0.6 for medium soil condition, and, finally, ω_g ranges from π to 3π (low frequency/high period) with $\xi_g = 0.2$ -0.4 for soft soil condition. Specific sampling techniques [47]-[52] are used to sample the data. Assuming the same duration [55],[56] equal to 31.25 s, longer than 25s as provided from [57], the Shinozuka-Sato function [58] is adopted as time-modulating function in order to define non-stationary stochastic processes for each set corresponding to each soil condition. Specifically, 100 artificial (non-stationary stochastic processes) records, generated through the Spectral Representation Method [30] and reflecting the wide uncertainty in terms of frequency content for each soil type [31],[54],[59] are defined for each soil condition.

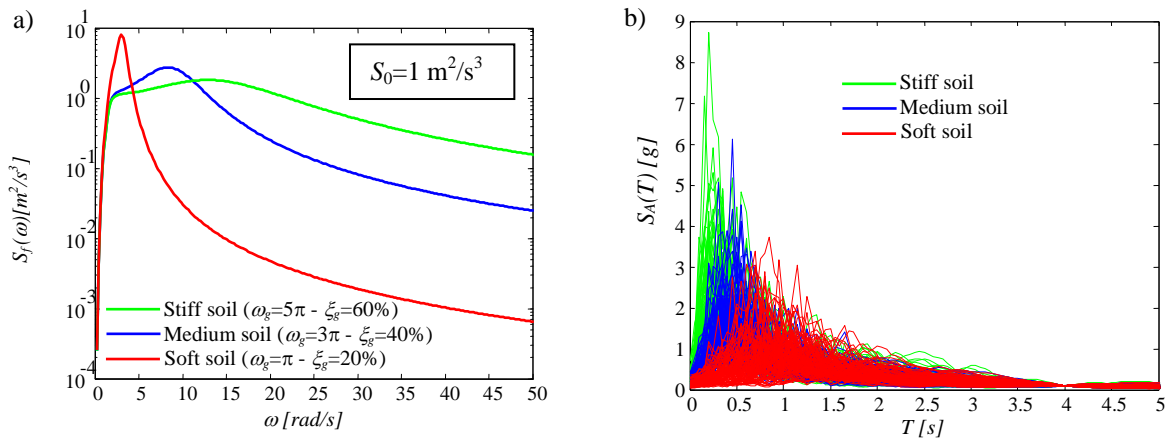


Figure 2: PSD functions corresponding to stiff, medium and soft soil conditions (a); Pseudo-acceleration response spectra for the 300 records scaled to the common seismic intensity measure $S_A(T) = 0.1$ g, for $T=4$ s (b).

Note also that, for each set of artificial records a high number of random excitations is defined in order to highly reduce the standard errors of the statistics of the response parameters [18]. As an example, Figs 2(a)-(b) show, respectively, the sampled PSD functions and the elastic pseudo-acceleration response spectra of the 300 artificial records, scaled to the common *IM* value $S_A(T) = 0.1g$, for a period $T = 4s$.

3.2 Intensity measure

In order to take into account the uncertainty related to the seismic intensity, the intensity scale factor, a_0 , of Eqn.(4), represents the seismic intensity measure (*IM*) in the context of the performance-based earthquake engineering (PBEE) [60],[61]. In this study, the abovementioned *IM* is denoted by the spectral pseudo-acceleration, $S_A(T_d, \xi_d)$, corresponding to the isolated period of the bridge $T_d = 2\pi / \omega_d$ with the damping ratio $\Pi_{\xi_d} = \xi_d$. Note that, in the analyses herein developed, the damping ratio ξ_d is set equal to zero [13],[23],[63] and the corresponding *IM* is hereinafter denoted as $S_A(T_d)$.

4 PARAMETRIC STUDY

This section describes the results of the parametric study carried out on the system of Figure 1 to evaluate the seismic performance of bridge isolated with FPS bearings for different structural properties and soil conditions. The first subsection describes the response parameters relevant to the seismic performance, whereas the final subsection illustrates the parametric study results. More details may be found in [62].

4.1 Non-dimensional response parameters relevant to the seismic performance assessment

The following response parameters relevant to the seismic performance assessment of isolated bridges are considered: the peak deck displacement relative to the pier $u_{d,max}$, the peak pier displacement $u_{p,max}$. These latter ones can be defined in non-dimensional form, as expressed in Eqn. (4), as:

$$\psi_{u_d} = \frac{u_{d,max} \omega_d^2}{S_A(T_d)} = \frac{u_{d,max}}{S_d(T_d)}, \quad \psi_{u_p} = \frac{u_{p,max} \omega_d^2}{S_A(T_d)} = \frac{u_{p,max}}{S_d(T_d)} \quad (8a,b,c,d)$$

For each soil condition (i.e., set of the 100 ground motion records), Eqn. (4) is repeatedly solved computing a set of samples for each response parameter. As also described in [13]-[22],[63]-[64], the response parameters are modeled in probabilistic terms by means of a lognormal distribution. Specifically, the generic response parameter D (i.e., the extreme values ψ_{u_d} , ψ_{u_p} of Eq. (4)) can be fitted by a lognormal distribution estimating the sample geometric mean, $GM(D)$, and the sample lognormal standard deviation $\sigma_{ln}(D)$, or dispersion $\beta(D)$, defined, respectively:

$$GM(D) = \sqrt[N]{d_1 \cdot \dots \cdot d_N} \quad (9)$$

$$\beta(D) = \sigma_{ln}(D) = \sqrt{\frac{(\ln d_1 - \ln[GM(D)])^2 + \dots + (\ln d_N - \ln[GM(D)])^2}{N-1}} \quad (10)$$

in which d_i is the i -th sample value of D , and N represents the total number of samples. The k th percentile of the generic response parameter D can be evaluated as:

$$d_k = GM(D) \exp[f(k)\beta(D)] \quad (11)$$

where $f(k)$ is a function that assumes the following values $f(50)=0$, $f(84)=1$ and $f(16)=-1$ [65], for the 50th, 16th and 84th percentile, respectively.

4.2 Parametric study results for each soil condition

In this section, the results of the parametric study developed using the proposed non-dimensionalization, for the different structural properties and for each set of 100 records, are illustrated and discussed. According to several studies [1]-[2],[4],[14]-[15],[29],[66]-[70], the parameters $\Pi_{\xi_d} = \xi_d$ and $\Pi_{\xi_p} = \xi_p$ are assumed respectively equal to 0% and 5%, the isolation period T_d varies in the range between 2s and 4s, the pier period T_p ranges from 0.05s to 0.2s, $\Pi_\lambda = \lambda$ varies between 0.1 and 0.2, Π_μ^* ranges between 0 (no friction) and 2 (very high friction) [13]. Other uncertainties [71]-[76] are not considered. Indeed, a high value for the upper bound of Π_μ^* is considered in order to take also into account the very low values of the IM at high isolated periods (i.e., $T_d=4$ s) depending on the seismic hazard [57]. For each parameter combination, the differential motion equations, i.e., Eqn. (4), have been repeatedly solved adopting the Bogacki-Shampine integration algorithm available in Matlab-Simulink [77]. After that, for each normalized response parameter, the geometric mean, GM , and the dispersion, β , have been evaluated through Eqns. (9) and (10) and are plotted in Figs. 5-12 for each soil type. Each figure contains several meshes, corresponding to the different Π_λ . The results for deck and pier displacements related to the all pier periods are reported.

Figs. 5-8 plot the results concerning the normalized deck displacement ψ_{u_d} , related to different pier period values. $GM(\psi_{u_d})$ is quite perfectly equal to unit for $\Pi_\mu^* = 0$ and $T_p = 0.05$ because of the very reduced influence of the pier behaviour. For $\Pi_\mu^* \neq 0$, and $GM(\psi_{u_d})$ increases slightly for increasing T_d because of the period elongation. Obviously, $GM(\psi_{u_d})$ decreases significantly as Π_μ^* increases while it is not heavily influenced by Π_λ . For soft soil condition and low Π_μ^* values, the decrease of $GM(\psi_{u_d})$ for increasing Π_μ^* is more gradual, while, for high Π_μ^* values $GM(\psi_{u_d})$ increases in the case of stiff soil, especially, for high T_p values due to the pier influence. The dispersion $\beta(\psi_{u_d})$ for high T_d increases for increasing values of Π_μ^* , as a result of the reduction of the efficiency of the IM employed in the study for each soil condition. Moreover, with reference to soft soils, the values of $\beta(\psi_{u_d})$ also result to be the highest for low or high values of both T_d and Π_μ^* . Obviously, in the reference situation corresponding to $\Pi_\mu^* = 0$ and $T_p = 0.05$ s, the dispersion is zero for all the values of T_d and of Π_λ considered and for all the soil conditions. The mass ratio Π_λ does not affect significantly the response dispersion, especially in the case of high T_p values.

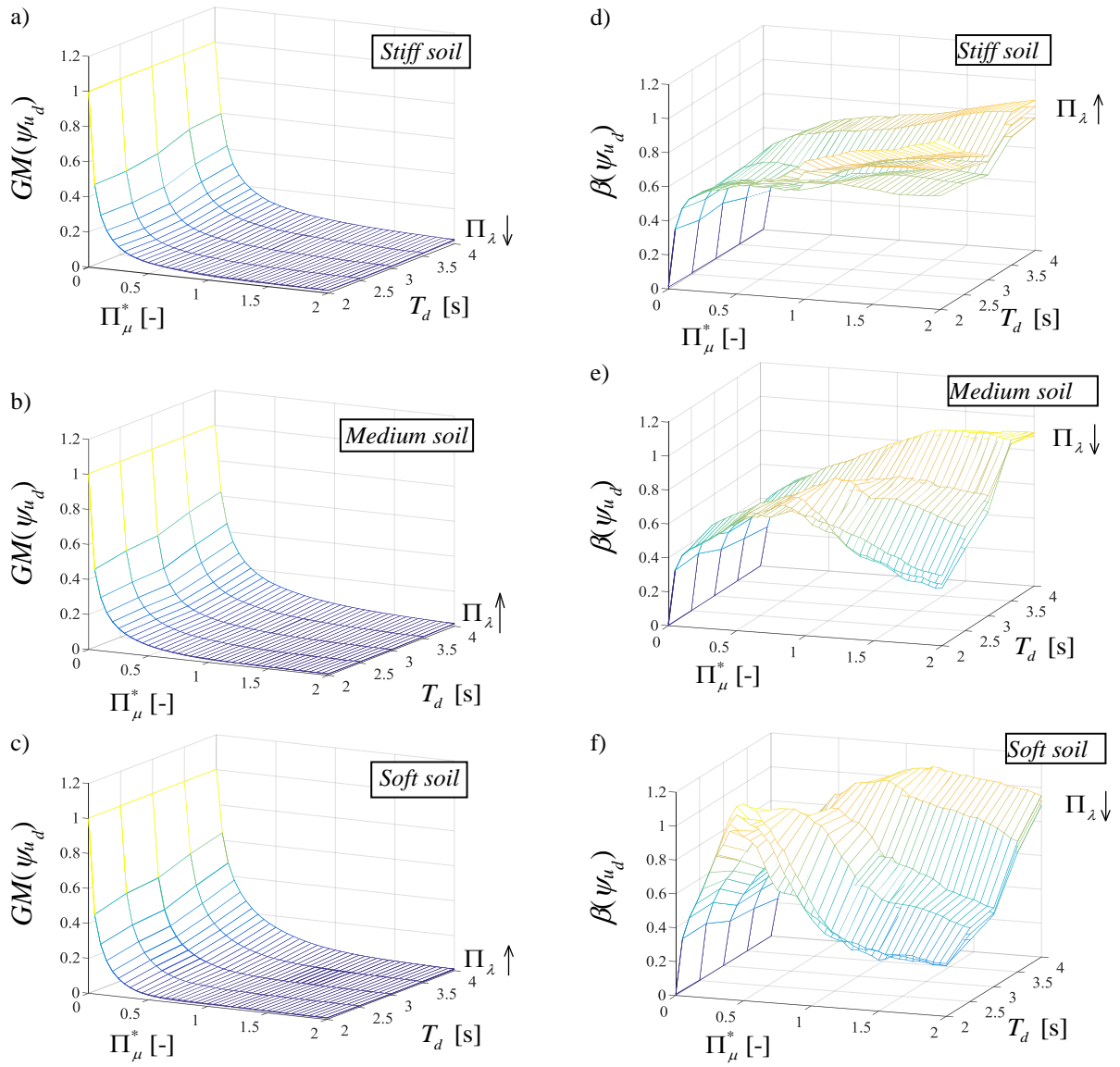
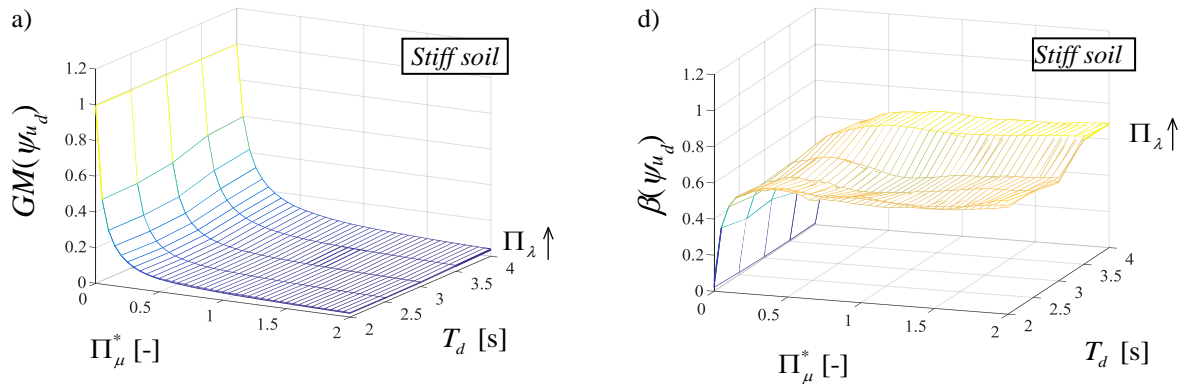


Figure 5: Normalized deck displacement vs. Π_μ^* and T_d for $T_p = 0.05$ s and each soil condition: median value (a,b,c) and dispersion (d,e,f) for different values of Π_λ . The arrow denotes the increasing direction of Π_λ .



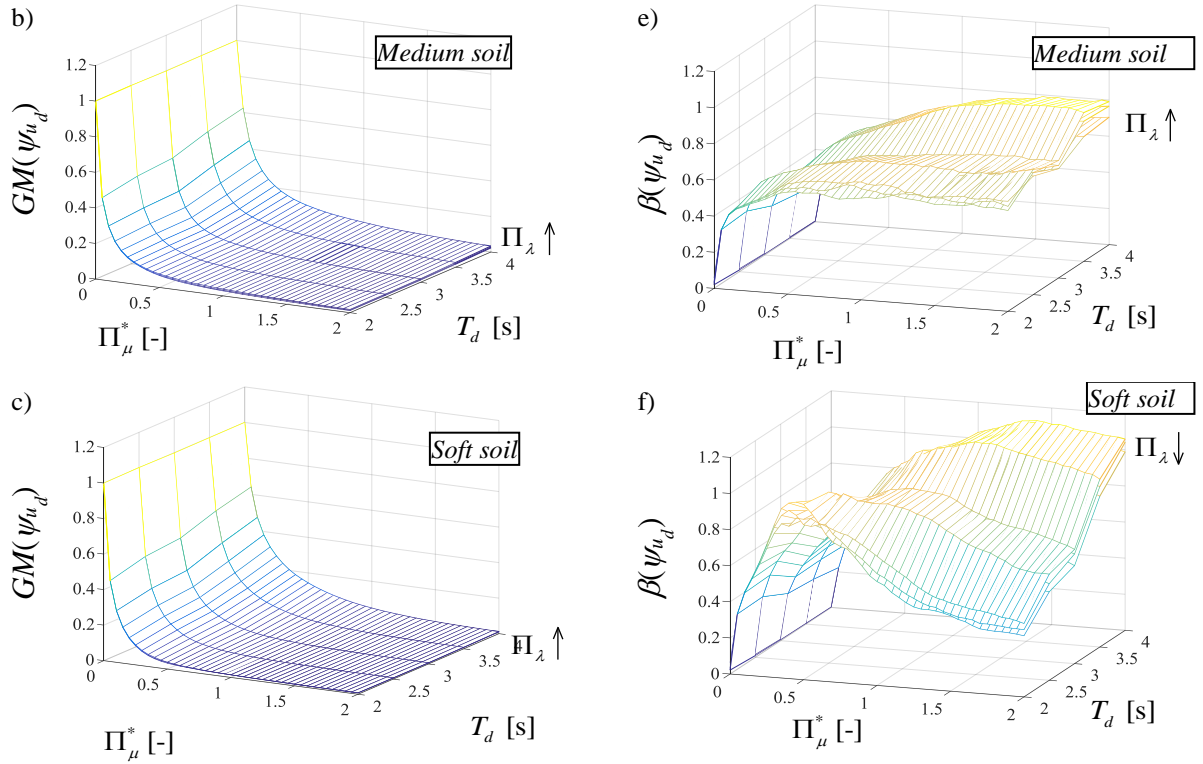
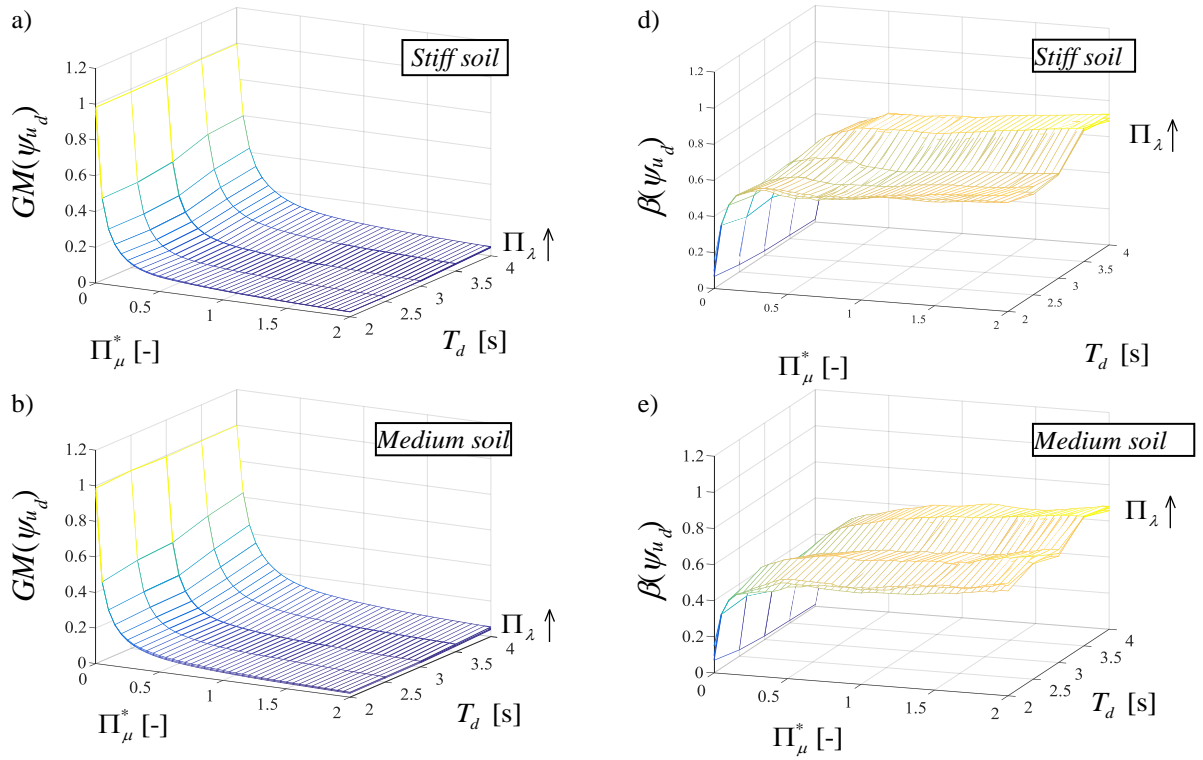


Figure 6: Normalized deck displacement vs. Π_μ^* and T_d for $T_p=0.1s$ and each soil type: median value (a,b,c) and dispersion (d,e,f) for different values of Π_λ . The arrow denotes the increasing direction of Π_λ .



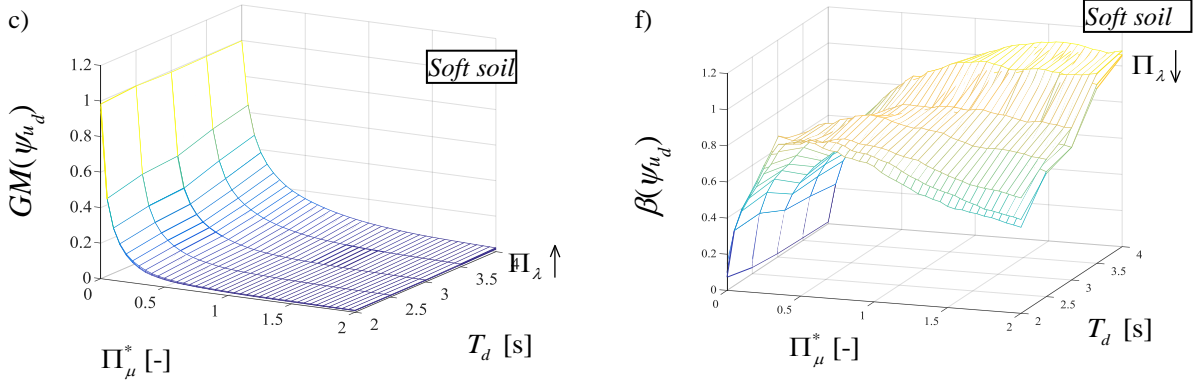


Figure 7: Normalized deck displacement vs. Π_μ^* and T_d for $T_p=0.15$ s and each soil type: median value (a,b,c) and dispersion (d,e,f) for different values of Π_λ . The arrow denotes the increasing direction of Π_λ .

The above described peak values of both $GM(\psi_{u_d})$ and $\beta(\psi_{u_d})$ in the case of soft soil condition are high due to the resonance effects which mainly affect the effective frequency characterizing the dynamic behaviour of the frictional bearings and the dominant frequency of the corresponding random excitations.

Figs. 8-12 show the response statistics of the normalized pier displacements ψ_{u_p} . $GM(\psi_{u_p})$ decreases for increasing values of T_d and of Π_λ as well as for decreasing values of T_p , whereas it first decreases and then increases for increasing values of Π_μ^* . Thus, this means that there exists an optimal value of the normalized friction coefficient Π_μ^* such that the pier displacement is minimized for each soil condition. This optimal value is in the range between 0.1 and 0.3 and depends on the values of T_p , T_d , Π_λ and on the soil condition. Differently to the case of base-isolated systems, there is not a particular and specific trend of the optimal friction coefficients from stiff to soft soil condition, as discussed later in detail. There is a further increase in the value of $GM(\psi_{u_p})$ from soft soil to stiff soil due to resonance effects, especially, for lower values of T_d . The values of the dispersion $\beta(\psi_{u_p})$ are very low for low Π_μ^* values due to the high efficiency of the *IM* used in this work, and attain their peak for values of Π_μ^* close to the optimal ones. The other system parameters have a reduced influence on $\beta(\psi_{u_p})$ compared to the influence of Π_μ^* . For the soft soil condition, the dispersion $\beta(\psi_{u_p})$ strongly increases for increasing values of Π_μ^* for low isolation period and for higher pier periods because of the resonance effects which mainly affect the effective frequency of the frictional bearings and the dominant frequency of the corresponding random excitations. As observed in similar studies [13],[23],[78]-[81], the existence of an optimal value of the friction coefficient derives from a combination of different effects. Indeed, an increase of the sliding friction coefficient leads to higher isolator strengths (and thus higher values of the equivalent stiffness, with a lowering of the corresponding effective fundamental vibration period (Fig.1)) and higher forces towards the deck. This also leads to an increase in the forces transmitted to the pier bridge due to inertial effect, relative to deck mass, on the pier.

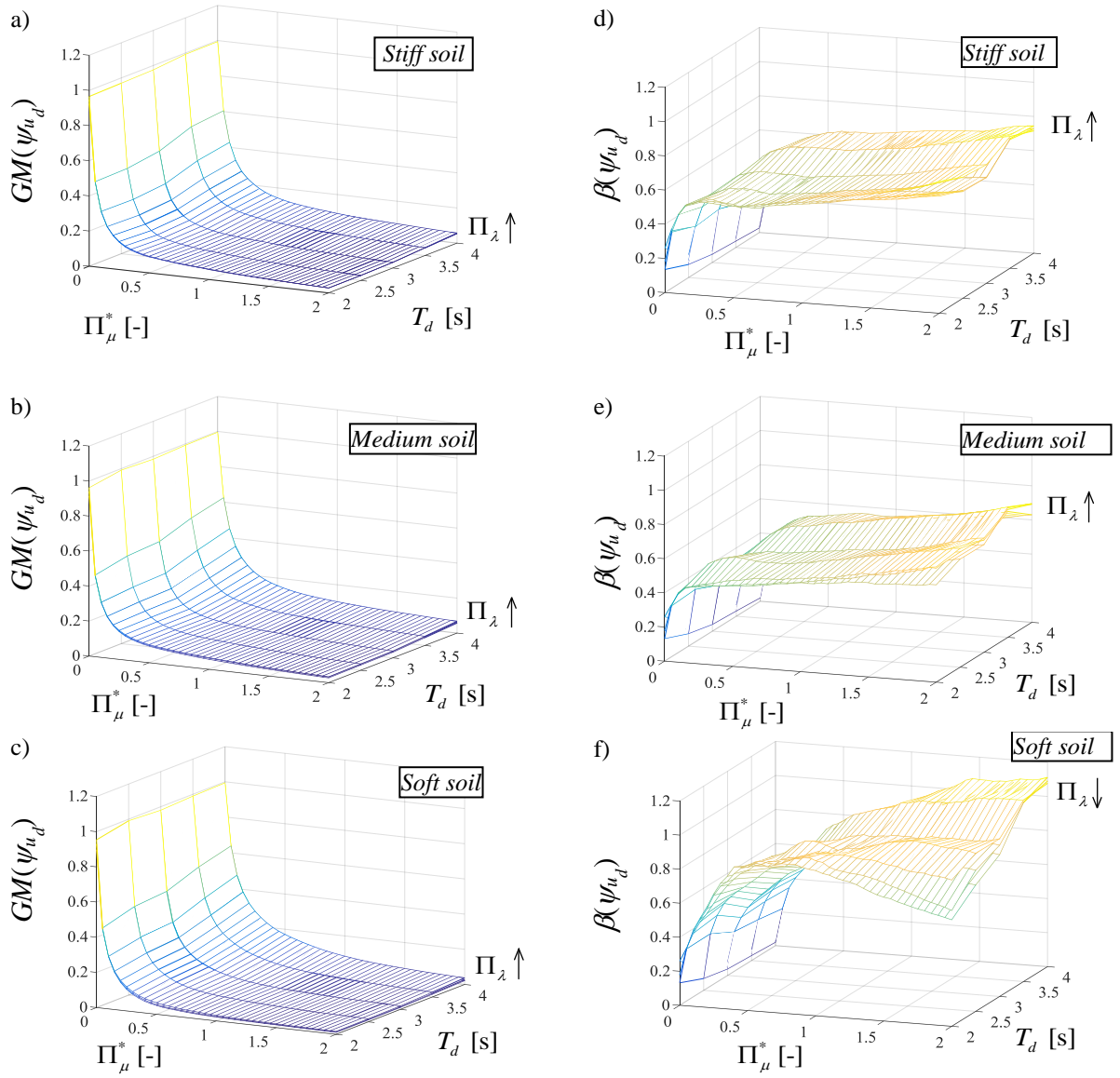
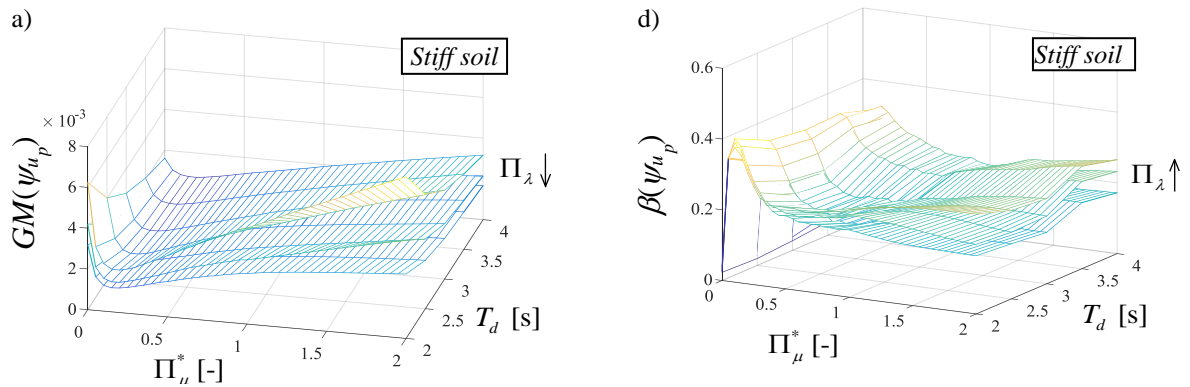


Figure 8: Normalized deck displacement vs. Π_μ^* and T_d for $T_p=0.2s$ and each soil type: median value (a,b,c) and dispersion (d,e,f) for different values of Π_λ . The arrow denotes the increasing direction of Π_λ .



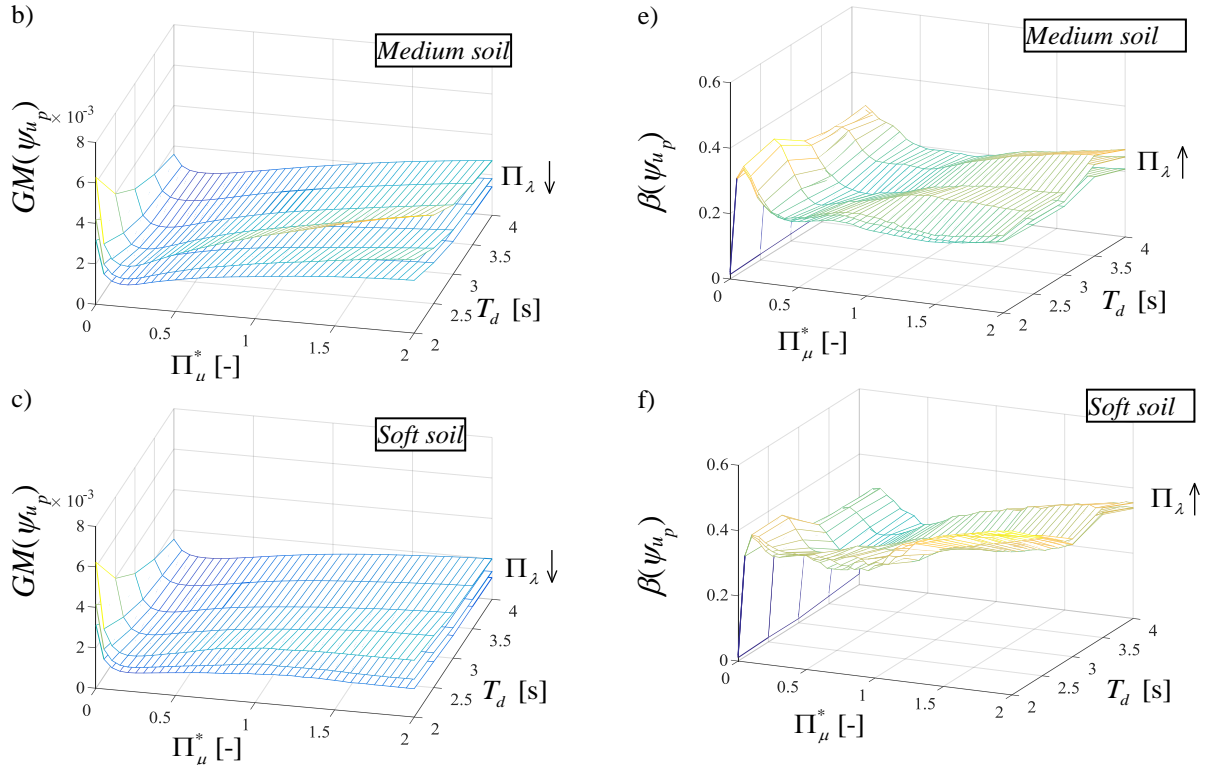
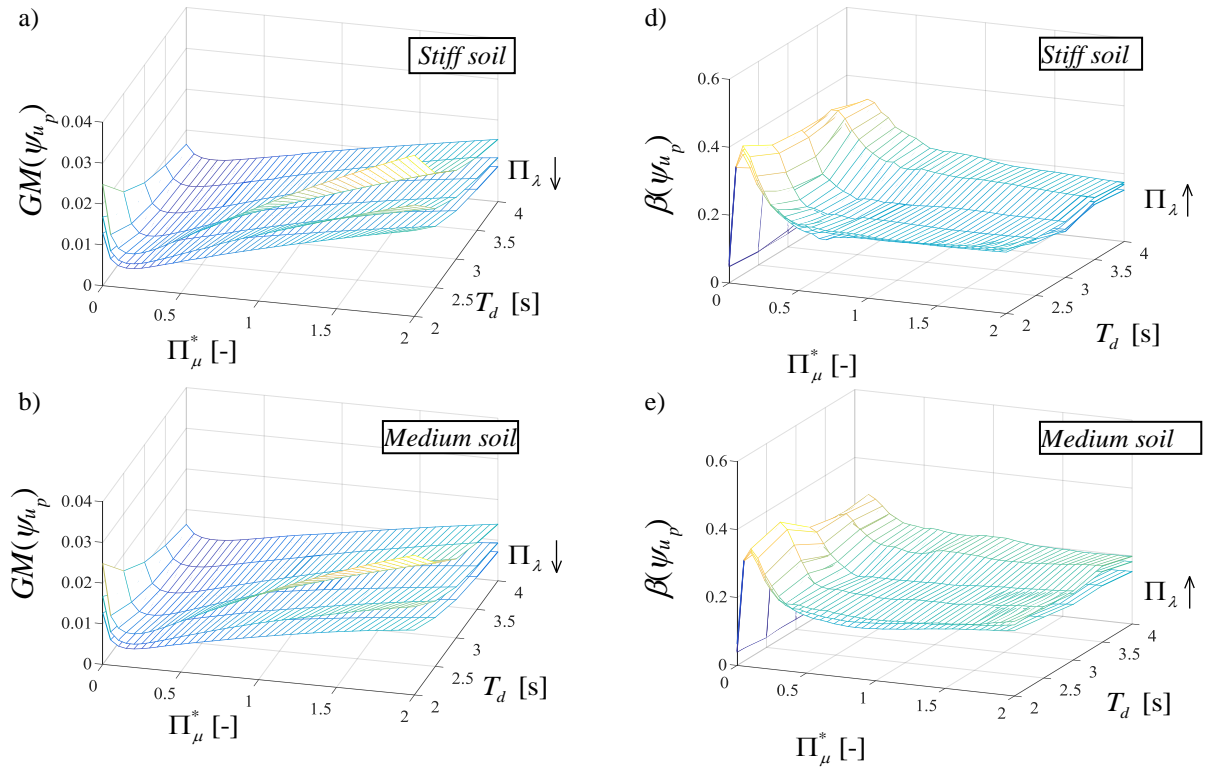


Figure 9: Normalized pier displacement vs. Π_μ^* and T_d for $T_p = 0.05s$ and each soil condition: median value (a,b,c) and dispersion (d,e,f) for different values of Π_λ . The arrow denotes the increasing direction of Π_λ .



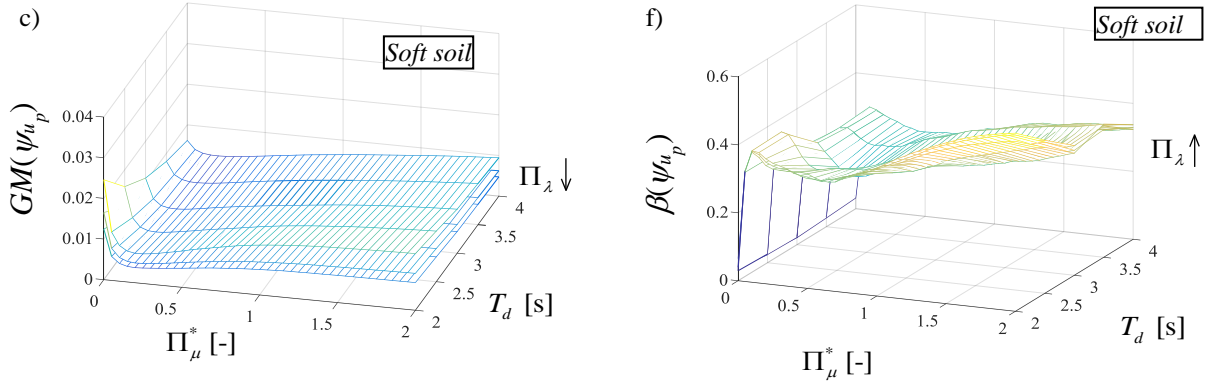


Figure 10: Normalized pier displacement vs. Π_μ^* and T_d for $T_p=0.1s$ and each soil condition: median value (a,b,c) and dispersion (d,e,f) for different values of Π_λ . The arrow denotes the increasing direction of Π_λ .

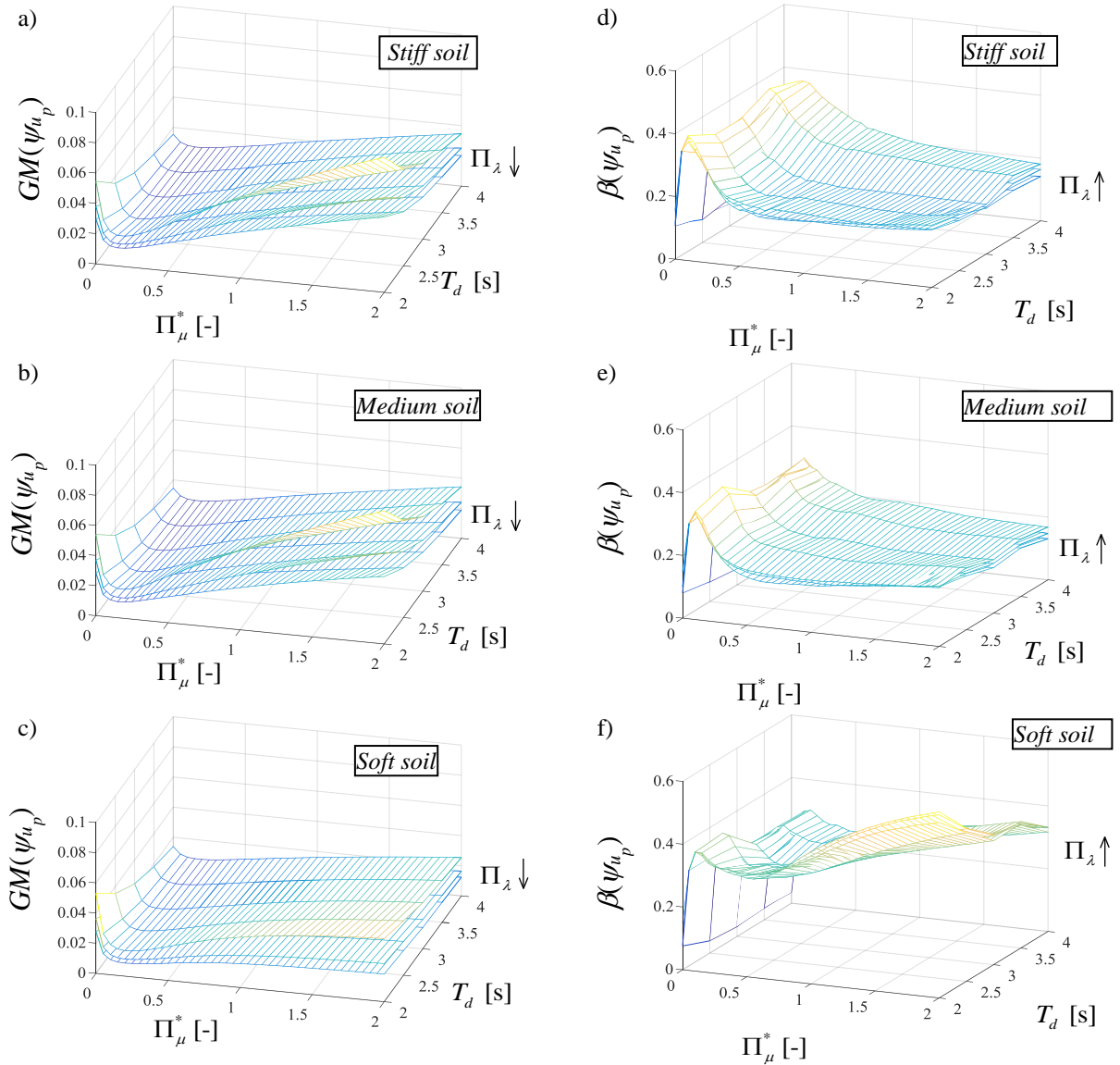


Figure 11: Normalized pier displacement vs. Π_μ^* and T_d for $T_p=0.15s$ and each soil condition: median value (a,b,c) and dispersion (d,e,f) for different values of Π_λ . The arrow denotes the increasing direction of Π_λ .

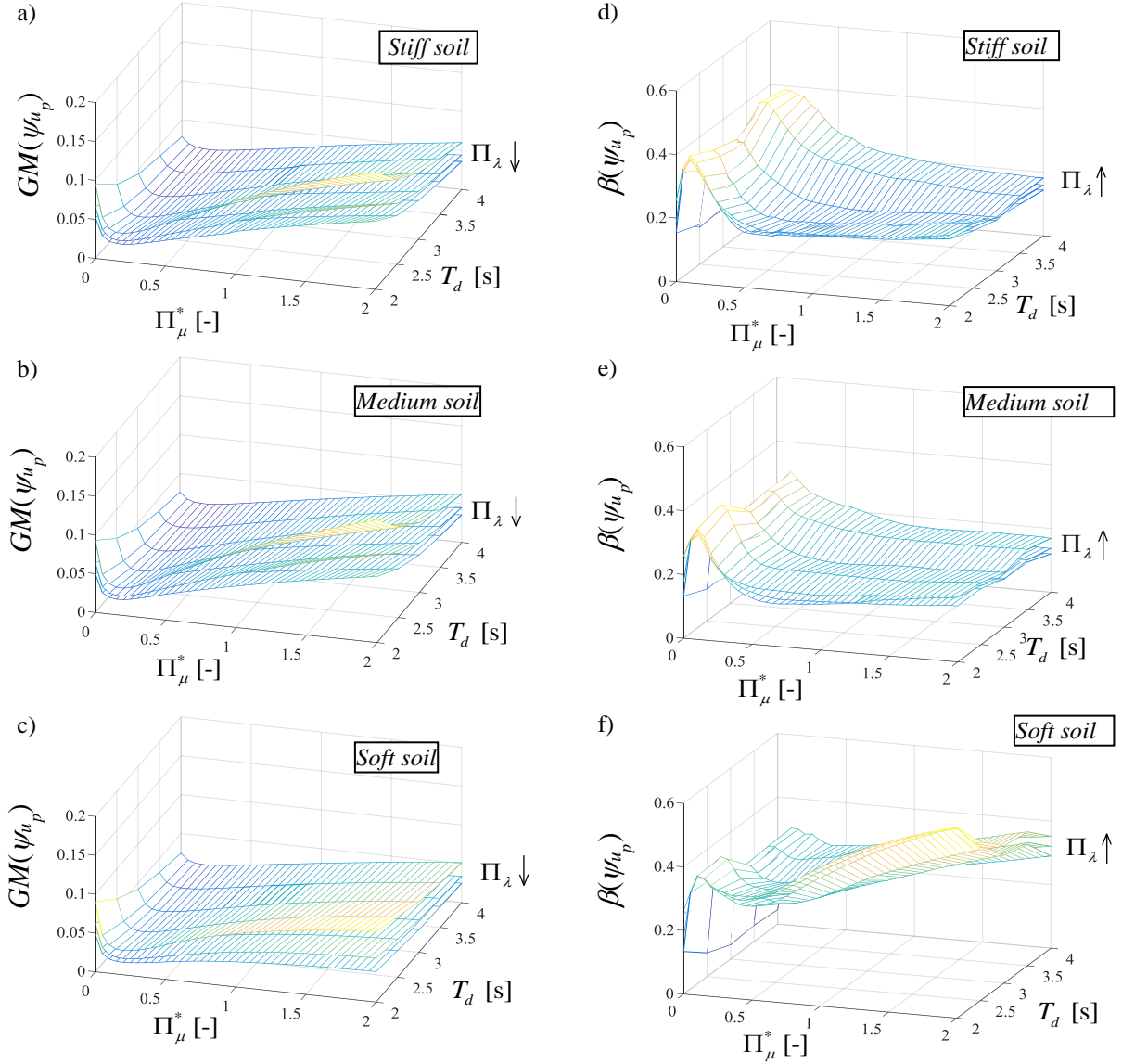


Figure 12: Normalized pier displacement vs. Π_μ^* and T_d for $T_p = 0.2s$ and each soil condition: median value (a,b,c) and dispersion (d,e,f) for different values of Π_λ . The arrow denotes the increasing direction of Π_λ .

However, the forces transmitted to the substructure also depend on the bearing displacements, which decrease as the friction coefficient increases. An increase of the forces transmitted to the substructure generally increases the substructure displacements. Contextually, another effect is the increase in terms of energy dissipation (equivalent damping), which reduces the substructure displacements. The balance between these effects defines the optimal friction coefficient of the FPS devices.

5 OPTIMAL SLIDING FRICTION COEFFICIENTS FOR ISOLATED BRIDGES DEPENDING ON SOIL CONDITIONS

From the results defined in the previous section, for each parameter combination (i.e., Π_λ , T_d and T_p) and soil condition, the optimal values of the normalized sliding friction coef-

ficient, $\Pi_{\mu, \text{opt}}^*$, that minimize the median (50th percentile) normalized pier displacements ψ_{u_p} have been computed and are illustrated in Fig. 13. Minimizing the pier displacements relative to the ground represents a notable design requisite for the safety of bridges in order to assure an adequate seismic protection. In fact, an inelastic response of the pier can lead to a disproportionately large displacement response that could also be amplified in the case of the resonance effects. Figure 13 shows the variation of $\Pi_{\mu, \text{opt}}^*$ with Π_λ and T_p for $T_d = 2\text{s}$ (Figure 13a,b,c) and $T_d = 4\text{s}$ (Figure 13d,e,f), for the three soil conditions.

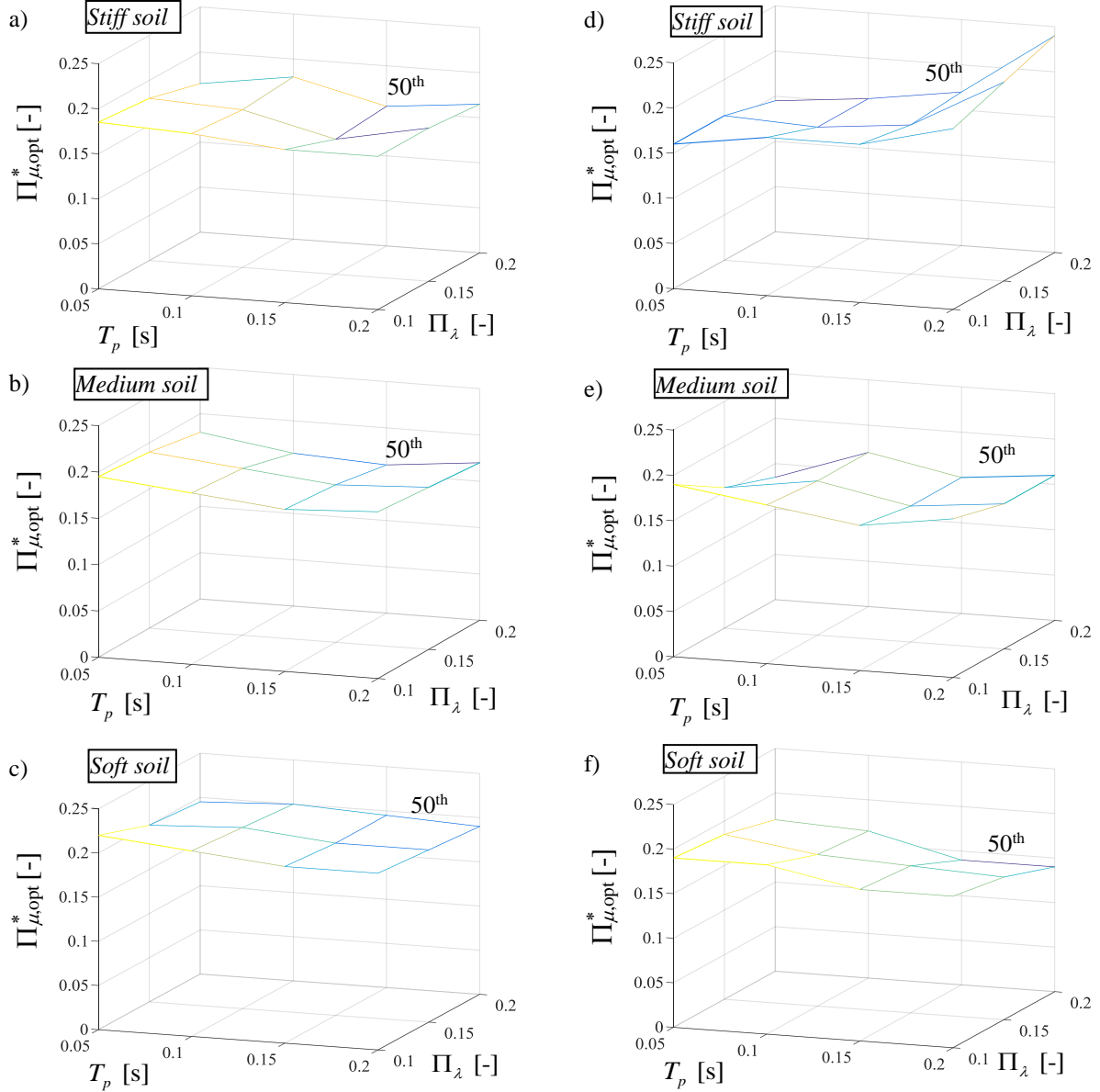


Figure 13: Optimal values of normalized friction that minimize the 50th percentile of the normalized pier displacements vs. Π_λ and T_p for each soil type and for $T_d = 2\text{s}$ (a,b,c) and $T_d = 4\text{s}$ (d,e,f).

According to [23], the optimal values of the (normalized) sliding friction coefficient slightly increase for decreasing T_d , especially for low T_p and for each soil condition. It is also observed that, for low T_d , $\Pi_{\mu, \text{opt}}^*$ generally decreases by increasing Π_λ and T_p . This trend is reversed with increasing of T_d and soil stiffness, when it is necessary to dissipate more energy, due to the resonance effects.

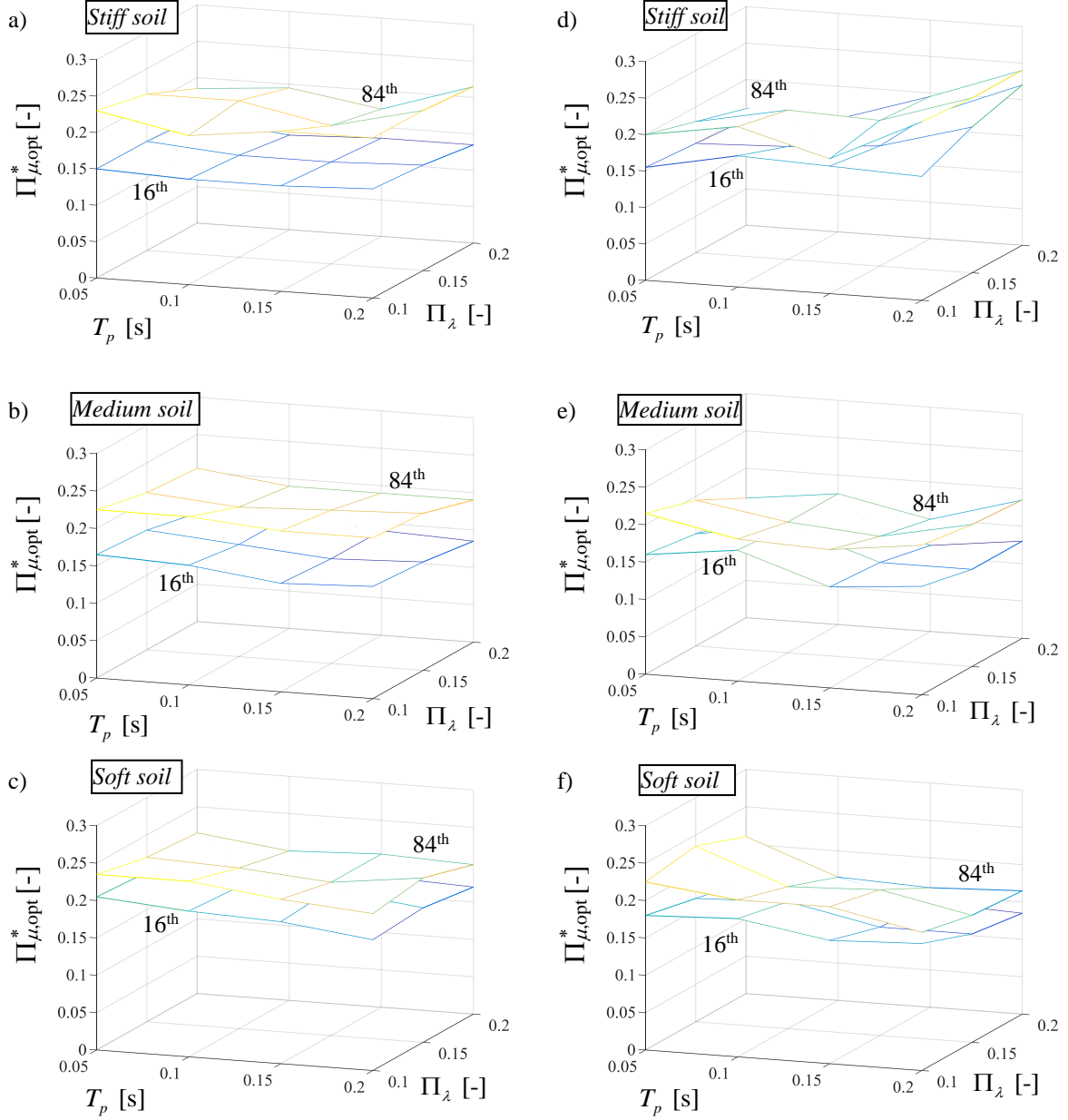


Figure 14: Optimal values of normalized friction that minimize the 84th and 16th percentiles of the normalized pier displacements vs. Π_λ and T_p for each soil type and for $T_d = 2\text{s}$ (a,b,c) and $T_d = 4\text{s}$ (d,e,f).

As previously discussed, it is also possible to observe that higher values of the optimum friction coefficient are required, especially for low isolated periods, for soft soil condition in order to reduce the bearing displacements and, consequently, the forces transmitted to the pier

as well as to increase the energy dissipation (equivalent damping). A reversal of this trend occurs for high values of both the isolation period and pier period, when it is necessary to dissipate more seismic energy input due to the resonance effect that affects the pier for stiff soil condition. In order to assure a high safety level, it might be of interest to define the values of $\Pi_{\mu, \text{opt}}^*$ that minimize others response percentiles [63]. Fig. 14 shows the optimal values of normalized friction that minimize the 84th and 16th percentiles of the normalized pier response for the different values of Π_λ , T_p , $T_d = 2\text{s}$ (Fig. 14a,b,c), $T_d = 4\text{s}$ (Fig. 14d,e,f) and for the three soil conditions. The trend is similar to the case of the 50th percentile. Regression expressions as statistics equations [82]-[87] to estimate the optimal friction coefficient may be found in [62].

6 CONCLUSIONS

This paper describes the seismic performance of elastic bridge pier equipped with friction pendulum system (FPS) bearings in order to define the optimal isolator friction properties as a function of the structural properties and of the soil characteristics in terms of frequency content, corresponding to stiff, medium and soft soils, respectively. Assuming an equivalent two-degree-of-freedom model, representative, respectively, of the dynamic behaviour of a single-column bent viaduct, describing a continuous and infinitely rigid deck with an elastic pier, and the velocity-dependent FPS isolator behaviour, a non-dimensionalization of the motion equations is herein proposed. For each soil type, the uncertainty in the seismic inputs is taken into account by means of a set of 100 artificial non-stationary stochastic records, obtained through the power spectral density method, with different frequency content. By means of the proposed non-dimensionalization, a wide parametric analysis is developed for several isolator and pier properties, and for different soil conditions, by monitoring the response parameters of interest.

With reference to the deck response, the geometric mean of the normalized deck displacement increases slightly for increasing isolation period because of period elongation and it decreases significantly as normalized friction increases while it is not heavily influenced by the mass ratio. The dispersion for high isolation period increases for increasing values of normalized friction. The mass ratio does not affect significantly the response dispersion, especially for high pier periods. There are resonance effects for soft soil condition and low normalized friction values, and for stiff soil condition and high normalized friction values, particularly, for higher values of the pier period.

With reference to the pier response, the geometric mean of the normalized displacement decreases for increasing values of isolation period and of mass ratio as well as for decreasing values of pier period, whereas it first decreases and then increases for increasing values of normalized friction. Thus, there exists an optimal value of normalized friction coefficient such that the pier displacement is minimized for each soil condition. This optimal value varies in the range between 0.1 and 0.3 depending on the system parameters and the soil type. The values of the dispersion are generally very low. The other system parameters have a reduced influence on the dispersion compared to the influence of the normalized friction. There are resonance effects for the stiff soil condition with increasing normalized friction values, particularly, for higher values of pier period and lower isolation period values.

REFERENCES

- [1] P. Tsopelas, M. C. Constantinou, S. Okamoto, S. Fujii, D. Ozaki. Experimental study of bridge seismic sliding isolation systems. *Engineering Str.*, Vol. 18, No. 4, pp. 301-310, 1996.
- [2] R.S. Jangid. Seismic Response of Isolated Bridges. *J. Bridge Eng.*, 2004, 9(2): 156-166.
- [3] A. Ghobarah and H. M. Ali. Seismic performance of highway bridges. *Eng. Struct.* 1988, Vol. 10, July.
- [4] N.P. Tongaonkar, R.S. Jangid. Seismic response of isolated bridges with soil–structure interaction. *Soil Dynamics and Earthquake Engineering* 23 (2003) 287–302.
- [5] Su L, Ahmadi G, Tadjbakhsh IG. Comparative study of base isolation systems. *Journal of Engineering Mechanic* 1989; **115**(9):1976–92.
- [6] Zayas VA, Low SS, Mahin SA. A simple pendulum technique for achieving seismic isolation. *Earthquake Spectra* 1990; **6**(2):317–33.
- [7] Mosqueda G, Whittaker AS, Fenves GL. Characterization and modeling of Friction Pendulum bearings subjected to multiple components of excitation. *J. of Str. Eng.* 2004; **130**(3):433-442.
- [8] Mokha A, Constantinou MC, Reinhorn AM. Teflon Bearings in Base Isolation. I: Testing. *Journal of Structural Engineering* 1990; **116**(2):438-454.
- [9] Constantinou MC, Mokha A, Reinhorn AM. Teflon Bearings in Base Isolation. II: Modeling. *Journal of Structural Engineering* 1990; **116**(2):455-474.
- [10] Constantinou MC, Whittaker AS, Kalpakidis Y, Fenz DM, Warn GP. Performance of Seismic Isolation Hardware Under Service and Seismic Loading. *Technical Report MCEER-07-0012*, 2007.
- [11] Almazàn JL, De la Llera JC. Physical model for dynamic analysis of structures with FPS isolators. *Earth. Engineering and Structural Dynamics* 2003;**32**(8):1157–1184.
- [12] Landi, L, Grazi G, and Diotallevi P P. Comparison of different models for friction pendulum isolators in structures subjected to horizontal and vertical ground motions, *Soil Dynamics and Earthquake Engineering* 2016;**81**:75-83.
- [13] Castaldo, P, Tubaldi, E. Influence of FPS bearing properties on the seismic performance of base-isolated structures. *Earthquake Engineering and Structural Dynamics* 2015;**44**(15):2817–2836.
- [14] Young-Suk Kim, Chung-Bang Yun. Seismic response characteristics of bridges using double concave friction pendulum bearings with tri-linear behaviour. *Eng. Str.*, 2007, 29:3082–3093.
- [15] Murat Eröz, Reginald DesRoches. Bridge seismic response as a function of the Friction Pendulum System (FPS) modeling assumptions. *Eng. Str.*, 2008, 30: 3204–3212.
- [16] Castaldo P, Palazzo B, Della Vecchia P. Seismic reliability of base-isolated structures with friction pendulum bearings. *Engineering Structures* 2015;**95**:80-93.
- [17] Castaldo P., Palazzo B., Della Vecchia P. Life-cycle cost and seismic reliability analysis of 3D systems equipped with FPS for different isolation degrees, *Engineering Structures*, 2016;**125**:349–363, <http://dx.doi.org/10.1016/j.engstruct.2016.06.056>.

- [18] Castaldo P., Amendola G., Palazzo B. Seismic fragility and reliability of structures isolated by friction pendulum devices: Seismic reliability-based design (SRBD), *Earthquake Engineering and Structural Dynamics*, 2017; 46(3); 425–446, DOI: 10.1002/eqe.2798.
- [19] Castaldo P., Palazzo B., Ferrentino T., (2016) “Seismic reliability-based ductility demand evaluation for inelastic base-isolated structures with friction pendulum devices”, *Earthquake Engineering and Structural Dynamics*, DOI: 10.1002/eqe.2854.
- [20] Castaldo, P., Mancini, G., Palazzo, B. (2018) Seismic reliability-based robustness assessment of three-dimensional reinforced concrete systems equipped with single-concave sliding devices, *Engineering Structures* 163, 373-387.
- [21] Castaldo, P., Palazzo, B., Alfano, G., Palumbo, M.F. (2018) Seismic reliability-based ductility demand for hardening and softening structures isolated by friction pendulum bearings, *Structural Control and Health Monitoring* 25(11),e2256.
- [22] Palazzo B, Castaldo P, Della Vecchia P. Seismic reliability analysis of base-isolated structures with friction pendulum system, 2014 IEEE Workshop on Environmental, Energy and Structural Monitoring Systems Proceedings, Napoli, September 17-18, 2014.
- [23] Jangid RS. Optimum friction pendulum system for near-fault motions. *Engineering Structures* 2005;**27**(3):349-359.
- [24] Dicleli, M., & Buddaram, S. Effect of isolator and ground motion characteristics on the performance of seismic-isolated bridges. *Earthquake Engineering and Structural Dynamics* 2006;**35**(2):233-250.
- [25] Safak, E., Frankel, A. Effects of ground motion characteristics on the response of base-isolated structures. *11th World Conference on Earthquake Engineering 1996* (paper no. 1430).
- [26] Saritaş, F, Hasgür Z. Dynamic Behavior of an Isolated Bridge Pier under Earthquake Effects for Different Soil layers and Support Conditions, *Digest* 2014, 1733-1756.
- [27] Wai-Fah Chen and Lian Duan. Bridge Engineering Handbook - Second edition. Seismic design. *Taylor & Francis Group*. 2014.
- [28] Castaldo, P., Tubaldi, E. (2018). Influence of ground motion characteristics on the optimal single concave sliding bearing properties for base-isolated structures. *Soil Dynamics and Earthquake Engineering*, 104: 346–364.
- [29] Masoud Malekzadeh, Touraj Taghikhany. Multi-Stage Performance of Seismically Isolated Bridge Using Triple Pendulum Bearings. *Advances in Str. Engineering* Vol. 15 No. 7, 2012.
- [30] Shinozuka M., Deodatis G. Simulation of stochastic processes by spectral representation. *Applied Mechanics Reviews* 1991;**44**(4):191-203.
- [31] Pinto P, Giannini R, Franchin P. Seismic Reliability Analysis of Structures. *Iuss Press* 2004.
- [32] Kelly JM. *Earthquake-Resistant Design with Rubber*. 2nd ed. Berlin and New York: Springer-Verlag; 1997.
- [33] Building Seismic Safety Council. NEHRP Recommended Provisions: Design Examples FEMA 451 - Washington, D.C., August 2006.

- [34] Priestley, M.J.N., Seible, F., Calvi, G.M., Seismic design and retrofit of bridges. Wiley, 1996.
- [35] Karavasilis TL, Seo CY, Makris N. Dimensional Response Analysis of Bilinear Systems Subjected to Non-pulse like Earthquake Ground Motions. *Journal of Structural Engineering* 2011;**137**(5):600-606.
- [36] Barbato M, and Tubaldi E. A probabilistic performance-based approach for mitigating the seismic pounding risk between adjacent buildings. *Earthquake Engineering & Structural Dynamics* 2013;**42**(8):1203-1219.
- [37] Palazzo B. Seismic Behavior of base-isolated Buildings. Proceedings of the International Meeting on earthquake Protection of Buildings, Ancona, 1991.
- [38] Pradlwarter H. J., Schuier G. I., Dorka U. Reliability of MDOF-systems with hysteretic devices. *Engineering Structures*, 1998;**20**(8):685-691.
- [39] Tung ATY, Wang JN, Kiremidjian A, Kavazanjian E. Statistical parameters of AM and PSD functions for the generation of site-specific strong ground motions. *Proceedings of the 10th World Conference on Earthquake Engineering*, Madrid, Spain, 1992;**2**:867-872.
- [40] Kanai K. Semiempirical formula for the seismic characteristics of the ground. *Bulletin of earthquake research institute* 1957;**35**:309-325.
- [41] Tajimi H. A statistical method of determining the maximum response of a building structure during an earthquake. *Proc., 2nd World Conf. on earthquake Engineering* 1960;**II**:781-798.
- [42] Clough R.W., Penzien J.: Dynamics of Structures, 2nd edn. McGraw-Hill, New York; 1993.
- [43] Zentner I., Allain F., Humbert N., Caudron M. Generation of spectrum compatible ground motion and its use in regulatory and performance-based seismic analysis. *Proceedings of the 9th Internat. Conf. on Str. Dyn.s*, EURO DYN 2014 Porto, Portugal, 30 June - 2 July 2014.
- [44] Peng Y., Chen J., Li J. Nonlinear Response of Structures Subjected to Stochastic Excitations via Probability Density Evolution Method. *Advances in Structural Engineering*, 2014;**17**(6):801-816.
- [45] Li, C., Liu, Y. Ground Motion Dominant Frequency Effect On The Design Of Multiple Tuned Mass Dampers. *Journal of Earthquake Engineering*, 2004;**8**(1):89-105.
- [46] Lopez-Garcia, D., Soong T.T. Assessment of the separation necessary to prevent seismic pounding between linear structural systems. *Prob. Engineering Mechanics*, 2009;**24**:210-223.
- [47] Castaldo P, Gino D, Carbone VI, Mancini G. Framework for definition of design formulations from empirical and semi-empirical resistance models, *Structural Concrete*, 19(4), 980-987, 2018 <https://doi.org/10.1002/suco.201800083>.
- [48] Castaldo, P., De Iuliis, M. (2014) Effects of deep excavation on seismic vulnerability of existing reinforced concrete framed structures, *Soil Dynamics and Earthquake Engineering* 64, 102-112.
- [49] Castaldo, P., Palazzo, B., Perri, F. (2016) Fem simulations of a new hysteretic damper: The dissipative column, *Ingegneria Sismica*, 33(1), 34-45.

- [50] Castaldo, P., Calvello, M., Palazzo, B. (2013) Probabilistic analysis of excavation-induced damages to existing structures, *Computers and Geotechnics*, 53, 17-30.
- [51] Castaldo P, Gino D, Bertagnoli G, Mancini G. Partial safety factor for resistance model uncertainties in 2D non-linear finite element analysis of reinforced concrete structures, *Engineering Structures*, 176(2018), 746-762.
- [52] Castaldo, P., Jalayer, F., Palazzo, B. (2018) Probabilistic assessment of groundwater leakage in diaphragm wall joints for deep excavations, *Tunnelling and Underground Space Technology* 71, 531-543.
- [53] Tubaldi, E., Barbato, M., Ghazizadeh S. A probabilistic performance-based risk assessment approach for seismic pounding with efficient application to linear systems. *Structural Safety* 2012;36-37:14–22.
- [54] Talaslidis D.G., Manolis G.D., Paraskevopoulos E.A., Panagiotopoulos C.G. Risk analysis of industrial structures with hazardous materials under seismic input, 13th World Conference on Earthquake Engineering, Vancouver, B.C., Canada, August 1-6, 2004.
- [55] Hancock J, Bommer JJ. A state-of-knowledge review of the influence of strong-motion duration on structural damage. *Earthquake Spectra* 2006;22(3):827-845.
- [56] Hancock J, Bommer JJ. Using spectral matched records to explore the influence of strong-motion duration on inelastic structural response. *Soil Dynamics and Earthquake Engineering* 2007;27:291-299.
- [57] NTC08. Norme tecniche per le costruzioni. Gazzetta Ufficiale del 04.02.08, DM 14.01.08, Ministero delle Infrastrutture.
- [58] Shinozuka M, Sato Y. Simulation of nonstationary random process. *J. Engrg. Mech. Div.* 1967;93(1):11-40.
- [59] Armouti, N.S. Response of structures to synthetic earthquakes. *Emerging Technologies in Structural Engineering. Proc. of the 9th Arab Structural Engineering Conf.*, Nov. 29 – Dec. 1, 2003, Abu Dhabi, UAE, 331-340.
- [60] Aslani H, Miranda E. Probability-based seismic response analysis. *Engineering Structures* 2005;27(8):1151-1163.
- [61] Porter KA. An overview of PEER's performance-based earthquake engineering methodology. Proceedings, *Proceedings of the 9th International Conference on Application of Statistics and Probability in Civil Engineering (ICASP9)*, San Francisco, California, 2003.
- [62] Castaldo, P., Ripani, M., Priore, R.L. (2018) Influence of soil conditions on the optimal sliding friction coefficient for isolated bridges, *Soil Dynamics and Earthquake Engineering* 111, 131-148.
- [63] Ryan K, Chopra A. Estimation of Seismic Demands on Isolators Based on Nonlinear Analysis. *Journal of Structural Engineering* 2004;130(3):392-402.
- [64] Karavasilis T, Seo C. Seismic structural and non-structural performance evaluation of highly damped self-centering and conventional systems. *Eng. Structures* 2011;33(8):2248-2258.
- [65] Ang AHS, Tang WH. Probability Concepts in Engineering-Emphasis on Applications to Civil and Environmental Engineering. John Wiley & Sons, New York, USA; 2007.

- [66] Yen-Po Wang, Lap-Loi Chung, Wei-Hsin Liao. Seismic response analysis of bridges isolated with friction pendulum bearings. *Earth.Eng. & Str. Dyn.*, 1998; 27, 1069-1093.
- [67] M.C. Kunde, R.S. Jangid. Seismic behavior of isolated bridges: A-state-of-the-art review. *Electronic Journal of Structural Engineering*, 3 (2003).
- [68] Evan m. Lapointe. An investigation of the principles and practices of seismic isolation in bridge structures. *Department of Civil and Environmental Engineering*; 2004.
- [69] Michael D. Symans, Steven W. Kelly. Fuzzy logic control of bridge structures using intelligent semi-active seismic isolation systems. *Earth. Engng. Struct. Dyn.* 28, 37-60, (1999).
- [70] Jangid R.S. Stochastic response of bridges seismically isolated by friction pendulum system. *J. Bridge Eng.*, 2008, 13(4): 319-330.
- [71] Di Lauro, F., Montuori, R., Nastri, E., Piluso, V. (2019) Partial safety factors and over-strength coefficient evaluation for the design of connections equipped with friction dampers, *Engineering Structures*, 178, pp. 645-655.
- [72] Fusco, R., Montuori, R., Nastri, E., Piluso, V. Critical analysis of ultimate rotation formula for R.C. columns subjected to cyclic loadings (2018) *Engineering Structures*, 177, pp. 160-174.
- [73] Dell'Aglio, G., Montuori, R., Nastri, E., Piluso, V. A critical review of plastic design approaches for failure mode control of steel moment resisting frames (2017) *Ingegneria Sismica*, 34 (4), pp. 82-102.
- [74] Nastri, E., Vergato, M., Latour, M. Performance evaluation of a seismic retrofitted R.C. precast industrial building (2017) *Earthquake and Structures*, 12 (1), pp. 13-21.
- [75] Piluso, V., Montuori, R., Nastri, E., Paciello, A. Seismic response of MRF-CBF dual systems equipped with low damage friction connections (2019) *Journal of Constructional Steel Research*, 154, pp. 263-277.
- [76] Dell'Aglio, G., Montuori, R., Nastri, E., Piluso, V. Consideration of second-order effects on plastic design of steel moment resisting frames (2019) *Bulletin of Earthquake Engineering*.
- [77] Math Works Inc. MATLAB-High Performance Numeric Computation and Visualization Software. User's Guide. Natick: MA, USA; 1997.
- [78] Chung LL, Kao PS, Yang CY, Wu LY, Chen HM. Optimal frictional coefficient of structural isolation system. *Journal of Vibration and Control* 2013, Early view. DOI: 10.1177/1077546313487938.
- [79] Iemura H, Taghikhany T, Jain S. Optimum design of resilient sliding isolation system for seismic protection of equipments. *Bulletin of Eart. Engineering* 2007;5(1):85-103.
- [80] Bucher C. Probability-based optimization of friction-based seismic isolation devices. *Structural Safety* 2009;31(6):500-507.
- [81] Fallah, N., Zamiri G. Multi-objective optimal design of sliding base isolation using genetic algorithm. *Scientia Iranica A*, 2013;20(1):87-96.
- [82] Garzillo, Carmine; Troisi, Roberta (2015) Le decisioni dell'EMA nel campo delle medicine umane. pp.85-133. In *EMA e le relazioni con le Big Pharma - I profili organizzativi della filiera del farmaco* - ISBN:9788892102279 - G. Giappichelli

- [83] Nese, Annamaria; Troisi, Roberta (2018) Corruption among mayors: evidence from Italian Court of Cassation judgments. DOI:10.1007/s12117-018-9349-4. pp.1-26. In *TRENDS IN ORGANIZED CRIME* - ISSN:1084-4791 vol. agosto 2018
- [84] Troisi, Roberta; Golzio, Luigi Enrico (2016). Legal studies and organization theory: a possible cooperation. pp.1-23. In *Manageable cooperation?* - ISBN:0024667498 - *European Academy of Management, Convegno: 16th EURAM Conference*, Paris, 1-4 June (ISSN 2466-7498).
- [85] Troisi, Roberta; Guida, Vittorio (2018). Is the Appointee Procedure a Real Selection or a Mere Political Exchange? The Case of the Italian Health-Care Chief Executive Officers. DOI:10.5947/jeod.2018.008. pp.19-38. In *JOURNAL OF ENTREPRENEURIAL AND ORGANIZATIONAL DIVERSITY* - ISSN:2281-8642 vol. 7 (2).
- [86] Troisi Roberta (2012). Le risorse umane nelle BCC: lavoro e motivazioni al lavoro. pp.399-417. In *Progetto aree bianche. Il sistema del credito cooperativo in Campania* - ISBN:8865580526 vol. 1.
- [87] Golzio Luigi Enrico; Troisi Roberta (2013). "The value of interdisciplinary research: a model of interdisciplinarity between legal research and research in organizations". pp.23-38. In *JOURNAL FOR DEVELOPMENT AND LEADERSHIP* , vol. 2.